

# The orbital motion of $\gamma^2$ Velorum<sup>★</sup>

W. Schmutz<sup>1</sup>, J. Schweickhardt<sup>2</sup>, O. Stahl<sup>2</sup>, B. Wolf<sup>2</sup>, T. Dumm<sup>1</sup>, Th. Gäng<sup>2,3</sup>, I. Jankovics<sup>4</sup>, A. Kaufer<sup>2</sup>, H. Lehmann<sup>5</sup>, H. Mandel<sup>2</sup>, J. Peitz<sup>2</sup>, and Th. Rivinius<sup>2</sup>

<sup>1</sup> Institut für Astronomie, ETH-Zentrum, CH-8092 Zürich, Switzerland

<sup>2</sup> Landessternwarte Heidelberg Königstuhl, D-69117 Heidelberg, Germany

<sup>3</sup> STScI, 3700 San Martin Drive, Baltimore MD 21218, USA

<sup>4</sup> Gothard Astrophysical Observatory, H-9707 Szombathely, Hungary

<sup>5</sup> Thüringer Landessternwarte Tautenburg, Karl-Schwarzschild-Observatorium, D-07778 Tautenburg, Germany

Received 26 May 1997 / Accepted 11 July 1997

**Abstract.** We analyze the orbital motion of  $\gamma^2$  Velorum based on high resolution optical spectra obtained in 1995 and 1996. By combining our data with values from the literature we find a period  $P = 78.53 \pm 0.01$  d. We determine radial velocity semi-amplitudes  $K_{WR} = 122 \pm 2$  km s<sup>-1</sup> and  $K_O = 38.4 \pm 2$  km s<sup>-1</sup> for the Wolf-Rayet star and the O star, respectively. The given errors are the standard deviations of the results from individual lines.

The inclination of the system is  $i = 65^\circ$ . This result is obtained by combining  $M_O \sin^3 i$  from the orbital analysis with the mass  $M_O = 29 M_\odot$ , obtained from its luminosity and stellar evolution tracks. The mass of the Wolf-Rayet component is  $M_{WR} = 9 M_\odot$ .

Our O star velocity curve disagrees by 15  $\sigma$  from a previously published result. We have identified the reason for the disagreement in the failure to correct for the WR emission that affects the measurements of the absorption line centers. The correction could have introduced systematic errors that may be larger than the given precision of the amplitudes. However, we can set an upper limit of  $K_O < 50$  km s<sup>-1</sup> from uncorrected measurements. This yields an upper limit for the Wolf-Rayet mass of  $M_{WR} < 12 M_\odot$ .

We find systematic phase-shifts between the velocity curves of some emission lines. We also observe that some (but not all) emission lines deviate significantly in the 1995 data set from the line's orbital solution defined by the 1996 observations. These phenomena may indicate that the radial velocities of the emission lines could be subject to systematic distortions and that the errors of the orbital motion are larger than the internal precision given here.

**Key words:** binaries: spectroscopic – stars: early-type – stars: fundamental parameters – stars: individual:  $\gamma^2$  Vel – stars: Wolf-Rayet

Send offprint requests to: W. Schmutz

★ Based on observations collected at the European Southern Observatory at La Silla, Chile. ESO proposals Nr. 56.D-327 and 57.D-517.

## 1. Introduction

The system  $\gamma^2$  Vel (HR 3207, HD 68273, WC8+O8 III) contains the closest Wolf-Rayet star, WR 11 (van der Hucht et al. 1988).<sup>1</sup> Its radio flux is strong enough to be recorded at mm and cm wavelengths and therefore, the mass loss rate of the WR star is known accurately (Leitherer & Robert 1991). Due to its binary nature  $\gamma^2$  Vel is one of the few systems for which it is also possible to measure the mass of the WR star. Therefore,  $\gamma^2$  Vel is an important system for the calibration of the relation between the WR mass and the WR mass loss rate (Langer 1989). This relation is crucial for evolutionary calculations of the Wolf-Rayet phase.

In view of  $\gamma^2$  Vel's magnitude,  $V = 1.8$ , we would expect that its orbit had been measured accurately long ago. However, only 14 years ago, when Pike et al. (1983) published their orbit solution, they wrote: "To resolve an outstanding disagreement on the period of the WC8+O9 I spectroscopic binary  $\gamma^2$  Velorum, a number of archival plates has been retrieved and measured. A period of 78.52 days has been found, but differences with some other elements have now appeared with serious consequences for the masses of the components and impending analysis of the WR wind."

The analysis of Pike et al. (1983) has apparently been superseded by the work of Moffat et al. (1986). The results of Pike et al. (1983) and of Moffat et al. (1986) are contradictory and the latter solution was accepted as the more reliable because it is based on observations with a good coverage of the whole orbital period and because the resulting mass of the O star agreed better with the classification as a supergiant. The latest investigation of  $\gamma^2$  Vel's orbit is that of Stickland & Lloyd (1990), who analyzed IUE observations. Due to the relatively low S/N

<sup>1</sup> Conti & Smith (1972) classified  $\gamma^2$  Vel as WC8+O9I. They note that due to blending problems the luminosity class of the O star is uncertain. Schaerer et al. (1997) have revised the spectral type to WC8+O8 III. Their luminosity class is based on the the He II  $\lambda 4686$  absorption whereas Conti & Smith (1972) used the ratio 4089 Si IV/4143 He I.

of these data, their solution had RMS residuals inferior to previous results. Therefore, they concluded: “We cannot claim to have improved the situation with regard to the definitive orbital elements of  $\gamma^2$  Vel, and indeed, our support for a small velocity amplitude for the O star may be seen as simply muddying some already murky waters.”

Recently, the measured parallactic distance to  $\gamma^2$  Vel by the HIPPARCOS satellite has brought a new argument to the discussion of its orbit (van der Hucht et al. 1997; Schaerer et al. 1997). Due to the revised distance the primary has a lower luminosity than thought previously. Now, the situation is reversed: the mass of the Pike et al. (1983) solution is in better agreement with the revised luminosity of the O star.

In the present paper we address the orbital motion of  $\gamma^2$  Vel based on a large data set of new spectroscopic observations. The observations are described in the next section. In Sect. 3 we derive the period by combining our data with that of Perrine (1920) and Pike et al. (1983). In Sect. 4 and 5 we measure the orbital elements and in Sect. 6 we investigate a peculiarity revealed by our observations: a phase shift of the C III/IV  $\lambda 4650$  line complex. In Sect. 7 the inclination of the system is determined. In the last section, we compare our results with previous determinations and discuss systematic influences on the measured amplitudes.

## 2. Observations and data reduction

We have collected a total of 133 spectra in the blue wavelength region and 145 in the red, simultaneously recorded with the fiber fed Echelle spectrograph HEROS (Heidelberg Extended Range Optical Spectrograph) at the ESO 50 cm telescope. The light path is divided into a blue and red path after the Echelle grating, then cross-dispersed with a grating for each channel, and finally, the spectrum is recorded on two CCDs. The total wavelength coverage of the instrument is from 3500 Å to 8600 Å. Because of the dichroic beam splitter there is a gap of about 250 Å, centered at 5700 Å. During an observing night typically every 2 hours lamp spectra are recorded for flat fielding and wavelength calibration. The two pixel resolution is  $R = 20\,000$  with nominal accuracy and stability of the wavelength calibration of  $0.35 \text{ km s}^{-1}$  RMS (Kaufer et al. 1997). To verify these numbers in practice we have measured the radial velocities of interstellar Ca II  $\lambda 3934$  and Na I  $\lambda 5890$ . We find that the scatter in the red channel agrees with the nominal accuracy of the instrument with systematic drifts below  $\pm 0.2 \text{ km s}^{-1}$ . In the blue path the radial velocity drifts between  $13.6 \text{ km s}^{-1}$  and  $14.5 \text{ km s}^{-1}$  with a RMS deviation of  $0.5 \text{ km s}^{-1}$  (Fig. 1). Thus, our observations are more accurate than  $1 \text{ km s}^{-1}$ . The signal to noise ratio of the spectra is  $S/N \approx 100$  at 3600 Å and  $S/N > 250$  at 6000 Å. The Echelle ripples are removed with the flat-field lamp response. Remaining ripple signatures are of the order of 1%. The spectra are normalized by a spline fit through selected wavelength points, roughly separated by 250 Å. These points are chosen to be free of emission lines but in the blue wavelength region, we probably do not reach the true continuum level.

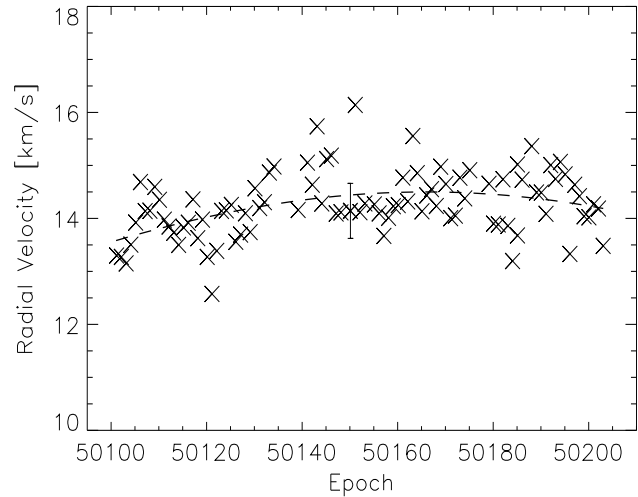


**Fig. 1.** Observed radial velocities of the interstellar Ca II  $\lambda 3934$ . The dashed line indicates a drift of the wavelength calibration and the error bar represents the RMS deviation of the data set. The epoch is given by JD-2,400,000.5.

The data were obtained in two observing runs from April 13 to June 2, 1995 and January 18 to April 30, 1996 (JD 2 449 821 to JD 2 449 871 and JD 2 450 101 to JD 2 450 204). We observed  $\gamma^2$  Velorum once a night with only few gaps. The data reduction was carried out by OS, AK, and TR based on a specially adapted version of the ESO-MIDAS Echelle context (Stahl et al. 1995).

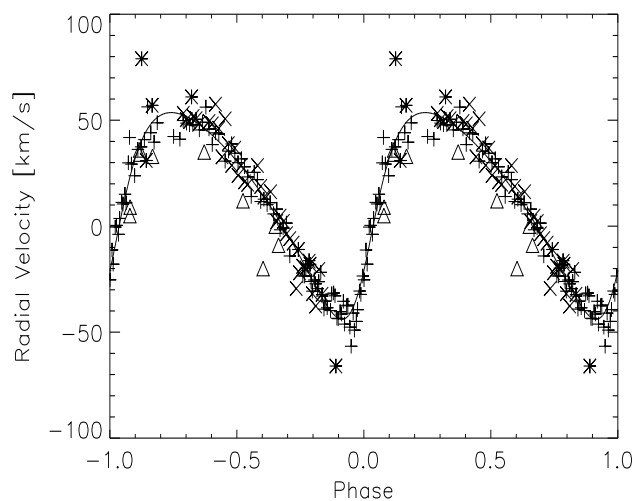
## 3. The orbital period

There are two papers comparing radial velocity data of  $\gamma^2$  Vel over a long time span. Pike et al. (1983) re-measured plates obtained between 1904 and 1913, and 1955 and 1959. They derive a period of  $P = 78.52 \pm 0.01$  days. Niemela & Sahade (1980) compare observations of 1919 with data from 1962. They find a phase shift of 3 days if  $P = 78.5 \text{ d}$  is assumed. From this difference they calculate a new period of  $P = 78.5002 \pm 0.0001 \text{ d}$ . However, their result is not correct. Between the observing dates there are only about 200 orbits, which yields  $P = 78.515 \pm 0.01 \text{ d}$ . Although we cannot reconstruct how they arrived at their conclusion, we note that Niemela & Sahade (1980) comment: “. . . orbital solutions for periods ranging between 78.49 and 78.53 days are compatible with our data, and neither one of them is completely ruled out.” In any case, if correctly calculated, the period of Niemela & Sahade (1980) is consistent with that of Pike et al. (1983).

In Fig. 2 we compare our orbital solution for the H9 absorption (Sect. 4.2) with absorption line velocities from the years 1904–1959. The data have been published by Pike et al. (1983). It is obvious that there is a shift of about  $10 \text{ km s}^{-1}$  between the velocity curve as defined by Thackeray’s data (triangles) and by our velocities. Luckily, the distribution of Thackeray’s data is such that the epoch of maximum radial velocity is nearly independent of the value of the systemic velocity. However, the older data of Mills expedition (stars) are sensitive to a differ-

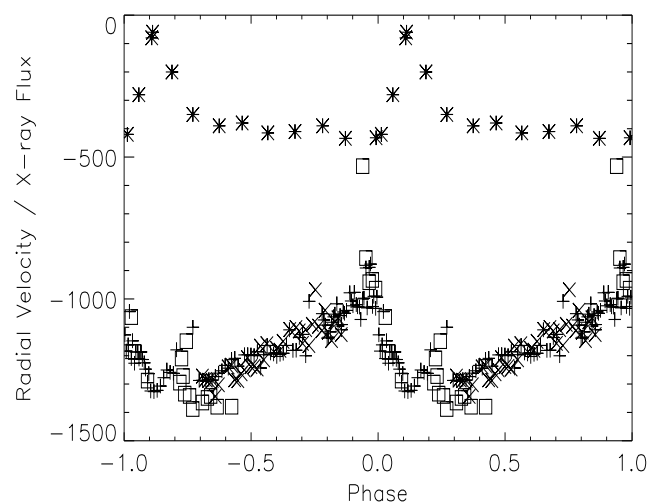
**Table 1.** Orbital elements determined from the radial velocity variations of different emission lines. A period of  $P = 78.53$  d is assumed and only the 1996 data are analyzed.

Parameter	C III/IV <sup>a</sup> $\lambda 4652$	C IV $\lambda 7730$	C IV $\lambda 4441$	C IV $\lambda 4786$	C III $\lambda 6740$	He II $\lambda 4686$	He II <sup>b</sup> $\lambda 4686$	He II <sup>b</sup> $\lambda 4860$
$\gamma^c$ [km s <sup>-1</sup> ]	–	-52.3	-12.9	109.8	-72.0	75.7	110.2	140.1
$e$	0.33	0.31	0.33	0.32	0.34	0.33	0.36	0.38
$\omega$ [deg]	66.6	71.8	68.1	69.0	66.1	64.5	55.1	78.1
$T_0$ JD 2,400,000.5+	50,118.1	50,121.7	50,121.2	50,121.6	50,118.6	50,120.5	50,118.9	50,117.5
$K$ [km s <sup>-1</sup> ]	122.2	119.8	125.2	118.1	125.4	110.5	123.5	137.4
$\sigma_{O-C}$ [km s <sup>-1</sup> ]	10.5	11.6	12.2	14.1	15.9	9.7	12.3	28.2

<sup>a</sup> Cross-correlation<sup>b</sup> Simultaneous double-Gauss fit to absorption and emission.<sup>c</sup> Reference wavelengths are: 7730.0, 4441.0, 4785.9, 6740.0, 4685.7, and 4859.3**Fig. 2.** Observed radial velocities of absorption lines. Crosses and plus signs denote measurements of H9 during 1995 and 1996, respectively. The stars represent mean absorption line velocities of H $\gamma$  through H10 obtained between 1904 and 1913 and the triangles indicate the values obtained between 1955 and 1959 (adopted from Pike et al. 1983). The line is the orbital solution fitted to the combined data set with a period  $P = 78.535$  days.

ence in  $\gamma$ -velocities and therefore, the Mills data set is of less value for the determination of the period. We derive a best fit of  $P = 78.535 \pm 0.01$  d, where the relatively large error allows for an unknown shift in systemic velocities between the data sets.

The radial velocities of the P Cygni absorption of He I  $\lambda 3889$  forms a saw-toothed pattern (cf. Fig. 1 of Niemela & Sahade 1980). Repeating the approach of Niemela & Sahade (1980), we compare our data with that of Perrine (1920) using a period of 78.5 d. We find a phase shift of 8 days. The time difference between the observations is 357 orbital periods and we obtain  $P = 78.522 \pm 0.005$  d. The error estimate is obtained by including the data set of Niemela & Sahade (1980) (see above). The problem with this method is that the P Cygni absorption is a feature formed in the wind. More exactly, we use the fast transi-

**Fig. 3.** Comparison of the variations of the observed velocity of the P Cygni absorption of He I  $\lambda 3889$  with the variation of the X-ray flux. Crosses and plus signs denote measurements of the P Cygni absorption during 1995 and 1996, respectively, and the squares mark the values reported by Perrine (1920). The velocities are measured in km s<sup>-1</sup> relative to the heliocentric rest-frame. The stars indicate the X-ray flux in units of milli-cts s<sup>-1</sup> shifted down by 500 milli-cts s<sup>-1</sup> (Willis et al. 1995).

tion from a slow wind to a fast wind around phase 0 to align the 1919 data with our data set. As shown in Fig. 3 this transition is exactly related to an increase of the hard X-ray flux (Willis et al. 1995). Therefore, the time dependence of the variation of the terminal velocity is probably related to the opening angle of the bow shock, similarly to the interpretation of the X-ray variability (Stevens et al. 1996). Such a phenomenon is likely to show cycle-to-cycle variations.

The two period determinations yield results that are only marginally consistent. We have identified reasons to suspect systematic effects in both approaches and therefore, the agreement is satisfactory. As we have no arguments to favor one method over the other we adopt the mean:  $P = 78.53 \pm 0.01$  d.

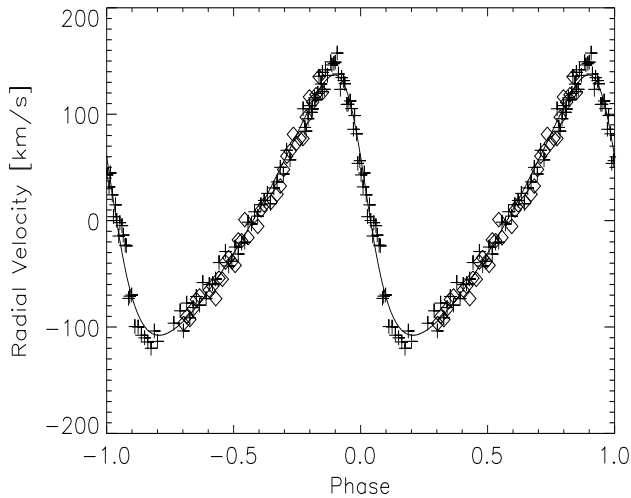


**Fig. 4.** Phase diagram of the radial velocities of the C III/IV line complex at 4650 Å. Plus signs denote our 1996 observations and the diamonds the 1995 data.

## 4. The velocity amplitudes

### 4.1. The emission lines

The emission lines have a full width at zero intensity corresponding to 3000 to 5000 km s<sup>-1</sup>. It is not straightforward to extract a velocity amplitude of 200 km s<sup>-1</sup> from lines of more than ten times this width. In order to measure the radial velocity we have fitted Gaussian profiles to the emission lines. The only exception is the line complex C III/IV  $\lambda$ 4650 Å which is not well represented by a Gaussian. We measured the line shifts of the C III/IV  $\lambda$ 4650 emission with a cross-correlation method. However, the main difficulty in measuring radial velocities arises not from the line widths but from the variability of the line shapes. Part of the line profile variations, such as the line widths, are clearly systematic. Other changes appear to be stochastic.

In Table 1 we summarize the orbital solutions obtained for individual emission lines. We minimize the sum of the squared deviations by varying simultaneously all free parameters. Besides the orbital elements the fit yields also the RMS deviation. We find that there are lines that show a higher degree of variability whereas others are fairly well behaved. We identified six lines that define the orbital motion with a RMS scatter of less than 20 km s<sup>-1</sup>. As an example we display in Fig. 4 the radial velocity curve of C III/IV  $\lambda$ 4650. In Table 1 we list an identification for the features but we do not attempt to derive the systemic velocity from these lines because the centers of the emissions are red-shifted by an amount that depends on the individual transition.

The RMS scatter of H $\beta$  is twice as large as for the other lines. The reason is that superimposed on the H $\beta$  emission there is a strong absorption feature that originates in the spectrum of the O star. We have fitted H $\beta$  simultaneously with two Gaussian profiles, one for the emission and the other one for the absorption. We show an example in Fig. 5. Although the fit to the red wing is not perfect the observed profile is reproduced nicely by

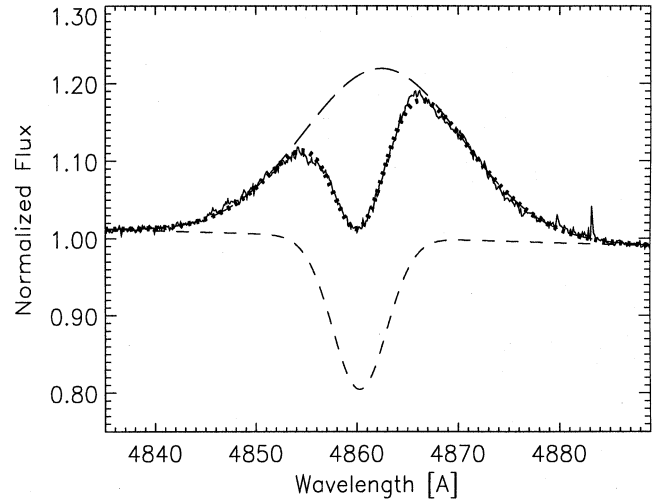


**Fig. 5.** Fit of a double-Gauss profile to the observed spectrum of H $\beta$ . The two Gauss-components are represented by the two dashed curves and the combined profile is indicated by dots.

the double-Gauss fit. It is not surprising that the radial velocities are more uncertain when two independent wavelength shifts and line strengths have to be determined simultaneously. However, it is essential to include the absorption feature when the radial velocities are measured. In order to demonstrate this point we have included in Table 1 two solutions for He II  $\lambda$ 4686: one obtained with a single-Gauss fit, the other with a double-Gauss fit. The amplitude from the single-Gauss solution disagrees on a 6  $\sigma$  level from the mean amplitude of the other lines. The relative strength of the absorption feature when compared to the emission is much less for He II  $\lambda$ 4686 than for H $\beta$ . Nevertheless, the He II  $\lambda$ 4686 absorption is sufficient to systematically shift the center of the emission feature such that a lower amplitude is measured. Niemela & Sahade (1980) and Moffat et al. (1986) have obtained a semi-amplitude for He II  $\lambda$ 4686 consistent with our single-Gauss fit. Both have omitted this line from the average orbital solution because “... this line often deviates in a similar way in other W-R binaries.” We now understand the reason for the odd behavior of this line. As demonstrated, the influence of the absorption can be corrected such that He II  $\lambda$ 4686 yields orbital elements that agree with those from lines that are free from absorption features.

As the deviation of the He II  $\lambda$ 4686 single-Gauss fit is systematic, we have excluded the elements of this solution from the average. We also exclude the He II  $\lambda$ 4860 result because due to the large correction for the relatively strong absorption, the elements for this line are more uncertain. With the six remaining solutions we determine a radial velocity semi-amplitude for the Wolf-Rayet star of  $\bar{K}_{WR} = 122$  km s<sup>-1</sup>. The six lines have an RMS error of 3 km s<sup>-1</sup>.

With about 50 measurements around the phases with maximal amplitude, each line solution yields an amplitude accurate to 1/7 of its RMS-scatter. Thus, we expect the semi-amplitudes of each individual solution to be accurate to 1.5 to 2 km s<sup>-1</sup>

**Table 2.** Orbital elements determined from absorption lines adopting  $P = 78.53$  d and  $e = 0.326$ . No correction for the influence of the WR emission is made.

Parameter	H9	H $\epsilon$	He I	H $\beta$	He I
	$\lambda 3835$	$\lambda 3970$	$\lambda 4471$	$\lambda 4861$	$\lambda 3889$
$\gamma$	13.2	4.2	-2.5	-14.6	6.0
$\omega$ [deg]	238.2	242.3	260.9	249.9	263.5
$T_0$ JD 2,400,000.5+	50,119.5	50,119.9	50,118.6	50,120.1	50,119.4
$K$ [km s $^{-1}$ ]	48.9	47.4	48.8	67.1	63.6
$\sigma_{O-C}$ [km s $^{-1}$ ]	5.6	5.6	10.9	13.5	9.9

(see Table 1). The standard deviation of the six values from the mean is larger than our estimates of the errors of the individual solutions. We suspect that there are systematic effects that we are not aware of and that the six results are not distributed randomly. Therefore, we refrain from reducing the error of the mean amplitude by a factor of  $\sqrt{6}$ , which would give an error of  $1.2 \text{ km s}^{-1}$ . Instead, we adopt the expected error of a solution for an individual line, i.e. we adopt  $\bar{K}_{WR} = 122 \pm 2 \text{ km s}^{-1}$ . With the quoted precision we have allowed for some of the systematic effects on the amplitude.

#### 4.2. The absorption lines

Within the wavelength coverage of our observations, all absorption features are blended by at least one emission line. In the simplest case of an absorption blended by the corresponding emission, the absorptions are superimposed on the steep sides of the WR emission during the phases of maximum radial velocity. The underlying slope of the emission shifts the line center towards the line wings. Measuring directly the center of the absorption features will overestimate the maximum positive as well as the maximum negative velocities. Thus, if no correction for the WR emission is made then inevitably too large amplitudes will be measured. In Table 2 we list the orbital elements obtained without correction for the emission blend. Depending on the strength and form of the WR emission we find velocity semi-amplitudes as large as  $67 \text{ km s}^{-1}$ . With the understanding that these values are too large, they yield an upper limit for the O star's velocity amplitude. We note that Niemela and Sahade (1980) and Moffat et al. (1986) have measured semi-amplitudes of  $70 \text{ km s}^{-1}$  and  $83 \text{ km s}^{-1}$ . From the upper limits of the uncorrected measurements in Table 2 we can qualify their results as being systematically too large. In particular, the results from He and H9, for which we find fit solutions with a very small intrinsic RMS scatter, set a very stringent upper limit to the orbital velocity of the O star:  $K_O < 50 \text{ km s}^{-1}$ .

Although it is clear that we must correct for the WR emission, it turns out that in practice this task is far from trivial. Some lines are blended by several other lines such that the blending problem is so severe that it is hopeless to define a reliable correction. Unfortunately, the two lines with the best RMS scatter belong to this category. Inspection of the wavelength regions around He and H9 reveals multiple line blends. We believe that

their good RMS scatter testifies to only small disturbances by WR features. However, we know that there are He II emissions at the wavelengths of the hydrogen absorptions, even though they cannot be isolated among the lines that contribute to the blends.

In order to take into account the WR emission we have tried several approaches. In Table 3 we give results obtained by double-Gauss fits and by subtracting a mean emission profile with the absorption removed shifted according to the WR orbital elements. In both cases we find that the intrinsic variations of the emission line profiles limit the accuracy of the results. This is obviously the case when we subtract a mean profile. But also the double-Gauss fit suffers from the variations because sometimes the line shapes are clearly less well reproduced by Gauss profiles. In addition, any correction is subject to systematic errors and we cannot exclude the possibility that our approach introduces systematically too large corrections. As we can only correct for isolated line emissions we are left with only five lines to derive the elements of the O star. We find  $\bar{K}_O = 38.4 \pm 2 \text{ km s}^{-1}$ , where we have given single weight to He I  $\lambda 4025$  and to the means of the two results for He I  $\lambda 4471$  and H $\beta$ , and a smaller weight for He II  $\lambda \lambda 4686, 5411$  corresponding to their squared RMS-deviation relative to that of the other lines. The given error is the standard deviation defined by the five results. In view of the difficulties in measuring the absorption-line amplitudes, an error of  $2 \text{ km s}^{-1}$  is uncomfortably small. However, we know no better method for deriving a more reliable error estimate. Again, as for the emission lines, we refrain from reducing the error by the square root of the number of measurements because we do not believe the results deviate randomly from the correct amplitude.

#### 5. The eccentricity, periastron date, and systemic velocity

The eccentricity is the only orbital element that can be determined without difficulty. The five emission lines without absorption blends listed in Table 1 yield consistently  $\bar{e}_{em} = 0.326 \pm 0.01$ . The average eccentricity resulting from the absorption-line solutions is  $\bar{e}_{abs} = 0.38 \pm 0.1$ . Thus, the value from the absorption lines is consistent with that from the emissions. However, we note that the absorptions yield a factor of 10 higher uncertainty. Therefore, we have adopted the mean eccentricity of the

**Table 3.** Orbital elements determined from absorption lines adopting  $P = 78.53$  d,  $e = 0.326$ , and  $\omega = 248^\circ$ . The influence of the WR emission is taken into account with method a, b, or c.

Parameter	He I/II <sup>a</sup> $\lambda 4025$	He I <sup>b</sup> $\lambda 4471$	He I <sup>c,d</sup> $\lambda 4471$	He II <sup>a</sup> $\lambda 4686$	H $\beta^a$ $\lambda 4861$	H $\beta^c$ $\lambda 4861$	He II <sup>a</sup> $\lambda 5411$
$\gamma$	31.1	-17.6	1.5	18.5	-11.3	-17.9	35.5
$T_0$ JD 2,400,000.5+	50,120.5	50,118.2	50,116.7	50,120.8	50,121.9	50,120.9	50,119.8
$K$ [km s <sup>-1</sup> ]	37.9	37.9	38.4	35.7	39.6	37.4	41.6
$\sigma_{O-C}$ [km s <sup>-1</sup> ]	10.7	10.5	8.8	26.5	11.3	11.9	16.8

<sup>a</sup> Simultaneous double-Gauss fit to absorption and emission.

<sup>b</sup> WR emission locally approximated by a straight line.

<sup>c</sup> Fit to the absorption after subtracting a mean WR profile shifted according to the WR solution.

<sup>d</sup> High negative velocities around phase 0.9 excluded.

emission lines for the analysis the absorption lines (Table 2 and 3).

From the emission lines we calculate a mean periastron angle of  $\omega = 68.3^\circ$ . The RMS error is  $2.3^\circ$  but the distribution of the values is definitely not random but rather bimodal. The individual periastron angles are probably influenced by systematic effects and therefore, we adopt an error that is large enough to include all results except that of the He II  $\lambda 4861$  line:  $\omega_{WR} = 68^\circ \pm 4^\circ$ . The absorption line solutions yield a large scatter for the periastron angle (cf. Table 2). If we adopt  $\omega_O = \omega_{WR} + 180^\circ$  we obtain RMS deviations that are only marginally larger than by using  $\omega$  as a free parameter. Hence, there is no reason to allow for periastron angle of the O star other than opposite to the WR star. We adopt  $\omega_O = 248^\circ$  in order to calculate the elements of the O star (Table 3).

The mean periastron date of both the emission and the absorption lines, is  $T_0 = 2\,450\,120.5$  (Table 1 & 3). The RMS error is 1.6 d but again, as it was the case for the periastron angle, the distribution is obviously bimodal. We adopt the mean and set an error that includes all values from the well defined solutions. In the next section we discuss the differences between individual solutions in more detail. The ephemeris for the time of periastron passage is thus

$$\text{JD(periastron)} = 2\,450\,120.5 + 78.53E. \quad (1)$$

In this paper all phases are calculated with Eq. 1.

For some applications it is preferable to give phases relative to the conjunction of the stars. The WR star is in front, i.e. mid eclipse if  $i = 90^\circ$ , 48 days after periastron passage, i.e. at phase  $\phi = 0.61$

$$\text{JD(WR in front)} = 2\,450\,168.5 + 78.53E. \quad (2)$$

The ephemeris given by Eqs. 1 and 2 differ from those of Moffat et al. (1986) in that their periastron date is 1.3 d late and their conjunction date is 1.9 d early. The periastron date of Niemela & Sahade (1980) is 2.9 d later than the date corresponding to Eq. 1.

In principle, we should be able to calculate the systemic velocity with the same accuracy as the amplitudes. However, it is

obvious (Table 3) that this is not the case. We believe that the explanation for the large scatter in the  $\gamma$ -velocities is partially due to incorrect normalization of the spectra and partially, due to wrong reference wavelengths. To understand the former we remind the reader that we measure wavelength shifts with absorption troughs that are very broad. The O star rotates with  $v_{\text{rot}} \sin i = 220$  km s<sup>-1</sup> (Baade et al. 1990), thus the lines have a width of five times the velocity amplitude with a flat line center. If the underlying continuum has a wrong slope then it is indeed possible to obtain shifts of the order of a few km s<sup>-1</sup>. The latter explanation is due to line blends. Two of the three lines in Table 3 that have well defined solutions are blends. Since we do not know the ratio of the line strengths of its components we cannot calculate the effective wavelengths of the blends. In order to derive the systemic velocity we simply calculate the mean and adopt RMS deviation of the five lines for the precision:  $\gamma = 7 \pm 23$  km s<sup>-1</sup>.

## 6. A phase shift of the C III/IV $\lambda 4650$ line complex

As noted in the previous section, the periastron dates of the emission line solutions show a clear bimodal distribution. The lines C IV  $\lambda \lambda 4441, 4786, 7730$  yield  $T_0 = 2\,450\,121.9$  whereas C III/IV  $\lambda 4650$  and C III  $\lambda 6740$  give  $T_0 = 2\,450\,118.9$ . The difference of three days is significant and as demonstrated in Fig. 6, the phase shift is obvious even to inspection by eye when the two data sets are plotted on top of each other.

We do not understand this phenomenon. For the C III  $\lambda 6740$  line we find an orbit solution that is in perfect agreement with the other three lines and in particular, with a periastron date of 2,450,121.9, if we modify the fit procedure by including the nearby He II  $\lambda 6683$  and use a fixed line width. This result indicates that for the C III  $\lambda 6740$  the phase shift may not be real. The periastron date of the He II  $\lambda 4686$  belongs to the group of early periastron dates as well. However, an inspection of its radial velocity curve reveals that for this line the early periastron date is only due to the periastron angle of the solution which differs considerably from the other solutions. Hence, the He II  $\lambda 4686$  does not belong to the lines with a phase shift.

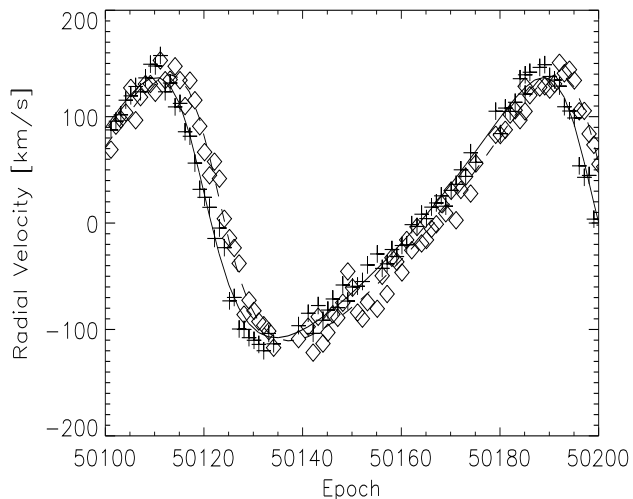


**Fig. 6.** Radial velocities of the carbon emission lines at 4650 Å (plus signs) and 4441 Å (diamonds). Both data sets have been shifted to zero systemic velocity. The orbital solutions given in Table 1 are indicated by the full line and the dashed line, respectively. The epoch is given by JD-2,400,000.5.

On the other hand, the shift of the strong C III/IV  $\lambda 4650$  appears to be real. We have tried several different approaches with multiple-Gauss fits and all combinations of fixed and variable line widths. We never obtain a significant deviation from the elements given in Table 1 and in particular, the data always show the phase shift when plotted against other transitions. Although the radial velocity curve of the He II  $\lambda 4860$  is not very well defined, it appears that also He II  $\lambda 4860$  shows a significant phase shift of about 4 days.

As a hypothesis we propose that the line profiles are disturbed by additional emission from the bow shock region. Hydrodynamical calculations of the collision of the WR wind with that of the O star predict a shock zone at the wind-wind interface. Because in the case of  $\gamma^2$  Velorum the momentum of the WR wind is much larger than that of the O star, the shock is wrapped around the O star and the flow directed fairly straight away from the WR, and with velocities of the order of the WR wind speed (see Fig. 2 of Walder 1995; Stevens et al. 1996). The proposed additional emission cannot be observed as an extra feature but it widens the line profiles in such a way that we measure an overall shift to the blue, when the stars are in conjunction and the WR is behind the O star, and to the red during the other conjunction when the WR star is in front. The line centers are not shifted during quadrature when we observe the highest radial velocities. Thus, the velocity amplitude is not altered.

According to our hypothesis we expect a systematic variation of the line width. Indeed, we observe that the line widths vary systematically with orbital phase. However, instead of two maxima of the line widths we only observe one. At least, the observations agree partially with our model, in that the maximum occurs during one of the conjunctions. We conclude that our model is too simple and that reality is more complex. Clearly,

a more elaborate investigation of this potentially interesting phenomenon is needed. Nevertheless, since in UV resonance lines there is clear evidence for colliding winds (St-Louis et al. 1993), it is well possible that the phase shift of at least the C III/IV  $\lambda 4650$  is real and due to additional emission not associated with the WR star. Additional evidence for emission possibly arising in a wind-wind collision zone was found by St-Louis (1996). She reported phase-related variability in the profile of C III  $\lambda 5696$ . The same type of profile variability is modeled successfully for WR 79 by Lührs (1997) with a simple model of the shock zone.

Similar phenomena are also observed in other WR binaries. Bertrand (1995) observed a line profile skewness in the case of WR 133. Moffat & Seggewiss (1977) found a phase shift close to a quarter period for the line C III  $\lambda 5696$  in  $\theta$  Mus. These observations are thought to be associated with effects of colliding winds.

## 7. The inclination

St-Louis et al. (1987) determined  $i = 70^\circ$  for the inclination of the  $\gamma^2$  Vel system. Their value is based on polarimetric observations but their analysis was based on an adapted eccentricity of  $e = 0.4$ . Since this value differs from our result, we have re-analyzed their polarization data using  $e = 0.326$ . In Fig. 7 we compare calculated Stokes parameters with the observed Q and U values. As St-Louis et al. (1987) we adopt the model of Brown et al. (1982) that assumes a point light source at the place of the O star and a scattering region localized at the WR star's position. We fit 7 free parameters by minimizing  $M = \sum \Delta_Q^2 + \Delta_U^2$ , where  $\Delta_Q = Q_{\text{obs}} - Q_{\text{cal}} - Q_0$  and the corresponding expression for  $\Delta_U$ . The best fit solution yields  $i = 68^\circ$ ,  $T_0 = 2\,450\,119.9$ ,  $\lambda_p = 140^\circ (+n \times 90^\circ)$ ,  $\Omega = 142^\circ (+180^\circ)$ ,  $\tau_* = 0.027$ ,  $Q_0 = 0.079\%$ , and  $U_0 = -0.087\%$  polarization. The epoch of the periastron passage,  $T_0$ , is in excellent agreement with the value derived by the radial velocity analysis. The fit is very sensitive to this parameter and we estimate an internal precision of about one day. The periastron angle is  $\omega = \lambda_p - 90^\circ = 50^\circ$ , which differs from the value  $\omega = 68^\circ$  derived from the radial velocities. However, the fit to the polarization data is not sensitive to that parameter and therefore, the difference is not significant.

We find that the changed eccentricity does not affect the resulting inclination. A comparison of Fig. 7 with Fig. 7 of St-Louis et al. (1987) reveals that our solution looks almost identical to their fit. The only apparent differences are the smaller amplitudes of our curves. The amplitude is parameterized by  $\tau_*$ , and consequently our value is considerably smaller than  $\tau_* = 0.045$  determined by St-Louis et al. (1987). The main reason that we obtain a different solution is that we do not include other polarization observations that are of inferior quality compared to the data of St-Louis et al. (1987).

The amplitude of the variation of the polarization depends on the number and distribution of the scatterers, i.e. the free electrons in the wind of the WR star. With the theory of St-Louis et al. (1988), that bases on the scattering model of Brown et al. (1978),

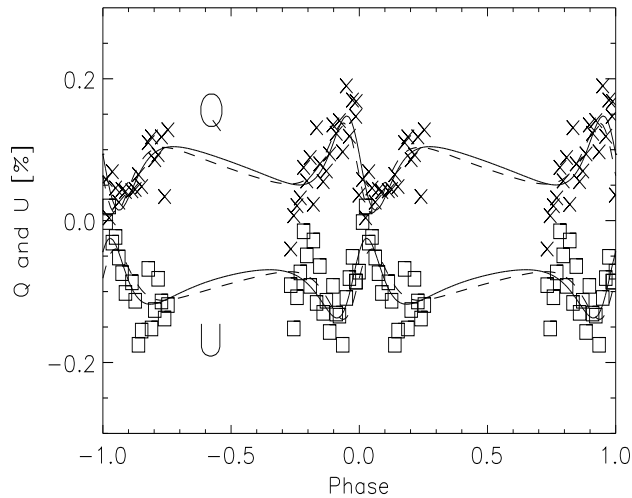


**Fig. 7.** Comparison of the observed Stokes parameters Q and U (St-Louis et al. 1987) with solutions calculated with a model assuming a localized scattering region associated with the WR star. The full drawn line marks the overall best solution with an inclination  $i = 68^\circ$  and the dashed curve represents the solution with  $i = 90^\circ$ .

it is possible to derive a mass loss rate. From our polarization fit we obtain a semi-major axis in the Q-U plane of  $A_p = 0.08$  % polarization. This value yields  $\dot{M} \approx 7 \cdot 10^{-6} M_\odot \text{yr}^{-1}$  (Eq. 6 of St-Louis et al. 1988). The interesting aspect of this number is that it is derived with a method that is proportional to the density. In contrast, the mass loss rate based on the interpretation of the radio flux depends on the density squared. Schaerer et al. (1997) calculate  $\dot{M} = 3 \cdot 10^{-5} M_\odot \text{yr}^{-1}$  with the HIPPARCOS distance, the mm and radio flux of Leitherer & Robert (1991) and Hogg (1985), and the terminal velocity of Eenens & Williams (1994). The ratio between the two mass loss determinations yields an estimate of the clumping in the WR wind. The numbers above imply a clumping factor of the order of 4, which agrees well with the factor 3 derived by Moffat & Robert (1994) from interpretations of line profile variations.

If it were only for the values given above it would be hardly worthwhile to report them. However, there is an important difference between our results and those of St-Louis et al. (1987). While they give a range  $50^\circ \leq i \leq 80^\circ$  we find that the published polarization data do not confine the inclination. In Fig. 8 we display the RMS-deviation of the best fits for given inclination. For all possible inclinations our solutions have a smaller RMS deviation than  $\sigma = 0.041$  % polarization reported by St-Louis et al. (1987) for their best fit.

Although we have improved the added squared deviations by 40% compared to the solution of St-Louis et al. (1987), our fit is still far beyond what we would expect for randomly distributed data points with the instrumental uncertainty. St-Louis et al. (1987) claim  $\sigma_{\text{inst}} = 0.013$  % polarization which seems to be correct judging from the accuracy they have obtained in the cases of measurements of other WR stars. With 82 measurements and 7 free parameters we expect  $\sigma = 0.013 \pm 0.001$  %. Thus, there is an effect of unknown origin that influences the

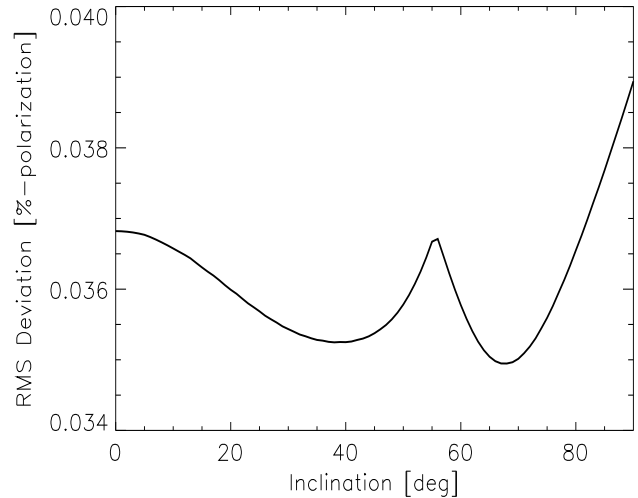


**Fig. 8.** Resulting RMS deviations of least squares fits to the observed Stokes parameters Q and U (see Fig. 7) as a function of the inclination.

observations. St-Louis et al. (1987) suspect a relation to the non-radial pulsations of the O star that are reported by Baade et al. (1990). Nevertheless, if we assume these deviations to be of random nature with  $\sigma = 0.035$  % polarization, which is the RMS deviation of our best fit, then we can also calculate a confidence range for the RMS deviation,  $\sigma = 0.035 \pm 0.0027$  % polarization. For the most unlikely inclination,  $i = 90^\circ$ , we calculate an RMS deviation of 0.039 % polarization. Thus, the fit with this inclination differs only by  $2\sigma$  from the best solution and has still a probability of 15% to be correct. This is demonstrated in Fig. 7 where we have also drawn the solution with  $i = 90^\circ$ . For an inspection by eye, both curves fit the data equally well. Obviously, the polarization observations are not accurate enough for a determination of the system's inclination.

A restriction of the system's inclination is possible from other considerations. Moffat (1977) did not find an eclipse in the continuum light curve. Therefore, we can set an upper limit to the inclination. With the radii<sup>2</sup>  $R_O = 13.2 R_\odot$  and  $R_{WR} \gtrsim 2 R_\odot$  (Schaerer et al. 1997) and the separation of the two stars,  $2a \sin i = 164 \cdot 10^6$  km (Table 4), we find  $i < 86.3^\circ$ .

Van der Hucht et al. (1997) and Schaerer et al. (1997) used the distance to  $\gamma^2$  Vel measured by HIPPARCOS, the period, and the observed angular separation of the binary components (Hanbury Brown et al. 1970) to derive the total mass of the system. They find  $M_{WR+O} = 29.5 \pm 15.9 M_\odot$ . The inclination resulting from the comparison with  $M_{WR+O} \sin^3 i$  derived here (Table 4) is  $i = 81^\circ$ . Because of the large uncertainty of the total mass, this inclination is not very precise. However, we obtain a lower limit  $i > 57^\circ$ .

From a spectral analysis of the O star Schaerer et al. (1997) derived its luminosity and then, by using single star evolutionary models, they obtain  $M_O = 29 \pm 4 M_\odot$ . The combination with our value for  $M_O \sin^3 i$  (Table 4) yields  $i = 65^\circ \pm 8^\circ$ . The quoted

<sup>2</sup> The WR radius refers to the Rosseland optical depth 30. The radius at  $\tau_R \approx 1$  is about  $6 R_\odot$ , which implies  $i < 85.3^\circ$ .

**Table 4.** Physical parameters of  $\gamma^2$  Velorum

$P$ [days]	78.53	$\pm 0.01$
mass ratio	0.31	$\pm 0.017$
$a_1 \sin i$ [ $10^6$ km]	39	$\pm 2$
$a_2 \sin i$ [ $10^6$ km]	125	$\pm 2$
$(M_1 + M_2) \sin^3 i$ [ $M_\odot$ ]	28.4	$\pm 1.6$
$M_O \sin^3 i$ [ $M_\odot$ ]	21.6	$\pm 1.1$
$M_{WR} \sin^3 i$ [ $M_\odot$ ]	6.8	$\pm 0.6$
$i$ [deg]	65	$\pm 8$
$M_O$ [ $M_\odot$ ]	29	$+8 -5$
$M_{WR}$ [ $M_\odot$ ]	9	$+2.5 -1.2$

error is an internal precision and does not include an uncertainty for the evolutionary tracks.

## 8. Discussion

In Table 5 we compare our orbital elements with previous determinations. For most parameters the present results are consistent with the earlier determinations except that the high quality of our observational data and the good coverage of the orbital period allows to tighten the errors. The only controversial values are the period and the velocity amplitude of the O star. We have pointed out in Sect. 3 that once the deviating value by Niemela & Sahade (1980) is recognized as due to a calculation mistake, all period determinations agree within their errors.

Regarding the radial velocity amplitude of the absorption lines we have identified the reason for disagreement. In Sect. 4.2 we have demonstrated that a direct fit to the absorptions without correcting for the influence of the WR emission leads to amplitudes as large as reported by Niemela & Sahade (1980) and Moffat et al. (1986). The semi-amplitudes of Ganesh & Bappu (1967) and Pike et al. (1983) agree with our new value. However, their papers do not mention that they have corrected for the influence of the WR emission. Therefore, the agreement is probably fortuitous.

In Sect. 6 we have reported a phase shift of the C III/IV  $\lambda 4650$  emission. Our interpretation of the phase shift is somewhat disturbing in view of a possible systematic influence on the accuracy of the other orbital elements. If the apparent periastron date can be shifted by additional emission from a region not associated with the WR star, what about the eccentricity and the amplitude? In fact, more in line with this expectation is the orbital curve of the He II  $\lambda 4860$ . If its radial velocities are plotted together with that of other lines then it is obvious that its deviating eccentricity is clearly significant. From the point of view that there is additional emission that disturbs the radial velocity, the most surprising result is that the orbital curve of the C III/IV  $\lambda 4650$  fits so perfectly with that of the other lines. For this line the only signature of the hypothetical influence is a phase shift.

The observations contain further unexplained effects that could influence the orbital solutions. We observe an erratic behavior of some lines (not all!) during our 1995 observations.

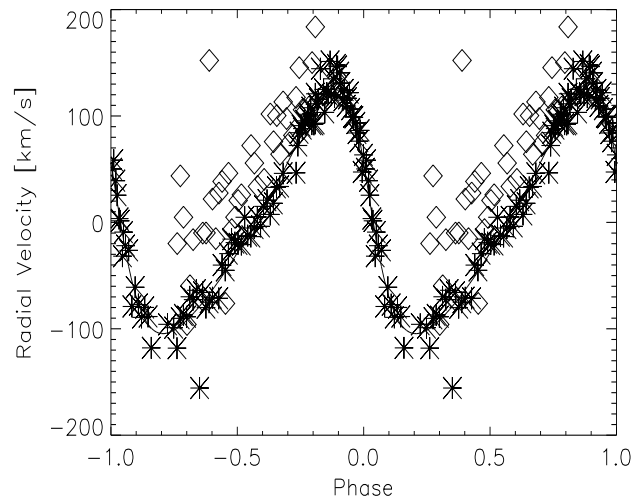


**Fig. 9.** Phase diagram for the radial velocities of C IV  $\lambda 4786$ . Stars denote our 1996 observations and the diamonds the 1995 data.

The most extreme case among the lines we have measured is C IV  $\lambda 4786$ . In Fig. 9 we show the phase diagram of this line. It is evident that the velocities from the 1995 observations are highly disturbed. Another example is C IV  $\lambda 4441$ . For the C IV  $\lambda 4441$  line we find a less extreme but still significant deviation of the 1995 data to more negative values than the orbit solution. The other lines listed in Table 1 do not show a disturbance. Their 1995 data are in perfect agreement with the 1996 observations in that both data sets yield the same distribution and RMS deviation from the orbital solution.

We note that despite the disturbing observations reported above we find consistent orbital elements from all lines, except for the periastron date and periastron angle. Therefore, the main results of our investigation, the velocity semi-amplitudes, appear not to be affected. Nevertheless, we cannot exclude that the systematic errors could be larger than the errors we report in Table 5. Unfortunately, we have no means to quantify our words of caution.

The most significant difference of the parameters derived here to previous determinations is the amplitude of the O star's orbit. We measure a value that is almost a factor of two smaller than that of Niemela & Sahade (1980) and Moffat et al. (1986). Consequently, we derive a much lower mass for the Wolf-Rayet star. Previously, it was commonly assumed that the WR star has a mass of  $M_{WR} \approx 20 M_\odot$ . With this mass the WR should have a luminosity of  $L = 10^{5.7} L_\odot$  (Smith et al. 1994), which is a factor of 10 higher than the luminosity obtained by the spectroscopic analysis of Schaerer et al. (1997). This disagreement is definitely too large. The mass implied by the WR's luminosity using the mass-luminosity relation for WR stars is  $M_{WR} \sim 5 \pm 1.5 M_\odot$  (Schaerer et al. 1997). This value is lower than the mass derived in the present analysis,  $M_{WR} = 9 M_\odot$ . However, Howarth & Schmutz (1992) find that the luminosities of Wolf-Rayet stars derived from their masses are systematically higher by about a factor of two than the luminosities obtained from spectroscopic

**Table 5.** Comparison of the orbital elements given in the literature with the present results.

Parameter	GB67	NS80	PSW83	MVPLB86	SL90	SSSW97	
$P$ [days]	78.5	78.515 <sup>a</sup>	78.52	...	...	78.53	$\pm 0.01$
$\gamma$ [km s <sup>-1</sup> ]	-18.0	12	5.7	...	-11	7	$\pm 23$
$e$	0.17	0.40	0.35	0.33 <sup>b</sup>	0.53	0.326	$\pm 0.01$
$\omega$ [deg.]	267	256	285	249	221	248	$\pm 4$
$T_0$ JD 2,400,000.5+	39,127.75	32,846.3	35,203.5	45802.4	43597	50,120	$\pm 2$
$K$ (abs) [km s <sup>-1</sup> ]	43	70	41	83 <sup>b</sup>	41	38.4	$\pm 2$
$K$ (emis) [km s <sup>-1</sup> ]	154	130	115	130	119	122	$\pm 2$

<sup>a</sup> NS80 give 78.5002 d. The entry is corrected for a calculation mistake.

<sup>b</sup> for their final solution MVPLB86 adopt  $e = 0.4$  and  $K = 70$  km s<sup>-1</sup> from NS80.

GB67: Ganesh & Bappu (1967); NS80: Niemela & Sahade (1980); PSW83: Pike et al. (1983)

MVPLB86: Moffat et al. (1986); SL90: Stickland & Lloyd (1990); SSSW97: this paper

analyses. Therefore, the disagreement between 5 and 9  $M_{\odot}$  is not unusual.

The most unfortunate aspect of the present investigation is that the determination of the inclination involves results from spectroscopic analysis and stellar evolution calculations. It would be preferable if fundamental stellar parameters could be used to test these calculations. We hope that in the future there will be sufficiently precise polarization observations to confine the inclination. We estimate that the polarization measurements need to be more precise than the existing data by about a factor of 5. The open question is whether there is intrinsic variability of the polarization that prevents results with this accuracy.

A long period system like  $\gamma^2$  Vel is not easy to observe. It was a considerable effort to obtain the observations presented in this paper. We were rewarded by a set of spectra of excellent quality that allowed us to measure the orbit of  $\gamma^2$  Vel with higher precision than before. Our results confirm the orbital elements obtained by Pike et al. (1983), but now we also understand the origin of the contradictory results obtained by Niemela & Sahade (1980) and Moffat et al. (1986).

*Acknowledgements.* We thank the staff at La Silla for their assistance. The construction of the spectrograph HEROS was supported by the Deutsche Forschungsgemeinschaft (Wo 296/20-1) and J.S. acknowledges the grant Wo 296/22-1. We thank Drs. A. Moffat, V. Niemela, and N. St-Louis for fruitful discussions and Drs. H. Nussbaumer and C. Lloyd for editorial comments.

## References

- Baade D., Schmutz W., van Kerkwijk M., 1990, A&A 240, 105  
 Bertrand J.F., 1995. In: van der Hucht K.A., Williams P.M. (eds.) Proc. IAU Symp. 163, Wolf-Rayet Stars: Binaries, Colliding Winds, Evolution. Kluwer, Dordrecht, p. 248  
 Brown J.C., Aspin C., Simmons J.F.L., McLean I.S., 1982, MNRAS 198, 787  
 Brown J.C., McLean I.S., Emslie A.G., 1978, A&A 68, 415  
 Conti P., Smith L.F., 1972, ApJ 172, 623  
 Eenens P.R.J., Williams P.M., 1994, MNRAS 269, 1082  
 Ganesh K.S., Bappu M.K.V., 1967, Kodaikanal Obs. Bull. Ser. A 183, 77

- Hanbury-Brown R., Davis J., Herbinson-Evans D., Allen L.R., 1970, MNRAS 148, 103  
 Howarth I.D., Schmutz W., 1992, A&A 261, 503  
 Hogg D.E., 1985. In: Hjellming R.M., Gibson D.M. (eds.) Radio Stars. Reidel, Dordrecht, 117  
 van der Hucht K.A., Hidayat B., Admiranto A.G., Supelli K.R., Doom C., 1988, A&A 199, 217  
 van der Hucht K.A., Schrijver H., Stenholm B., et al., 1997, New Astronomy 2, 245  
 Kaufer A., Stahl O., Wolf B., et al., 1997, A&A 320, 273  
 Langer N., 1989, A&A 220, 135  
 Leitherer C., Robert C., 1991, ApJ 377, 629  
 Lührs S., 1997, PASP 109, 504  
 Moffat A.F.J., 1977, A&A 57, 151  
 Moffat A.F.J., Robert C., 1994, ApJ 421, 310  
 Moffat A.F.J., Seggewiss W., 1977, A&A 54, 607  
 Moffat A.F.J., Vogt N., Paquin G., Lamontagne R., Barrera L.H., 1986, AJ 91, 1386  
 Niemela V.S., Sahade J., 1980, ApJ 238, 244  
 Perrine C.D., 1920, ApJ 52, 39  
 Pike C.D., Stickland D.J., Willis A., 1983, The Observatory 103, 154  
 Schaerer D., Schmutz W., Grenon M., 1997, ApJ 484, L153  
 Smith L.F., Meynet G., Mermilliod J.-C., 1994, A&A 287, 835  
 Stahl O., Kaufer A., Wolf B., et al., 1995, The Journal of Astronomical Data 1, 3 (on CD-ROM)  
 Stevens I.R., Corcoran M.F., Willis A.J., et al., 1996, MNRAS 283, 589  
 Stickland D.J., Lloyd C., 1990, The Observatory 110, 1  
 St-Louis N., 1996, Rev. Mex. Astron. Astrofis. (Ser. conf.) 5, 76  
 St-Louis N., Drissen L., Moffat A.F.J., Bastien P., Tapia S., 1987, ApJ 322, 870  
 St-Louis N., Moffat A.F.J., Drissen L., Bastien P., Robert C., 1988, ApJ 330, 286  
 St-Louis N., Willis A.J., Stevens I.R., 1993, ApJ 415, 298  
 Walder R., 1995. In: Wolf-Rayet Stars: Binaries, Colliding Winds, Evolution (IAU Symp. 163), eds. K.A. van der Hucht, P.M. Williams, Kluwer, Dordrecht, 420  
 Willis A.J., Schild H., Stevens I.R., 1995, A&A 298, 549

This article was processed by the author using Springer-Verlag L<sup>A</sup>T<sub>E</sub>X A&A style file L-AA version 3.